Mineralogical Magazine, June 2013, Vol. 77(3), pp. 429–441

Leydetite, $Fe(UO_2)(SO_4)_2(H_2O)_{11}$, a new uranyl sulfate mineral from Mas d'Alary, Lodève, France

J. Plášil[1,*], A. V. Kasatkin[2], R. Škoda[3], M. Novák[3], A. Kallistová[4], M. Dušek[1], R. Skála[4], K. Fejfarová[1], J. Čejka[5], N. Meisser[6], H. Goethals[7], V. Machovič[8,9] and L. Lapčák[8]

[1] Institute of Physics ASCR, v.v.i., Na Slovance 2, CZ-18221 Prague 8, Czech Republic
[2] V/O "Almazjuvelirexport", Ostozhenka Street, 22, block 1, 119034 Moscow, Russia
[3] Department of Geological Sciences, Faculty of Science, Masaryk University, Kotlářská 2, 4 611 37, Brno, Czech Republic
[4] Institute of Geology ASCR, v.v.i., Rozvojová 269, Prague 6, 16500, Czech Republic
[5] Department of Mineralogy and Petrology, National Museum, Cirkusová 170, CZ-193 00, Prague 9, Czech Republic
[6] Musée géologique cantonal and Laboratoire des rayons-X, Institut de minéralogie et de géochimie, Université de Lausanne, 1015 Lausanne-Dorigny, Switzerland
[7] Musée de l'Institut royal des sciences naturelles de Belgique, Section mineralogy, Rue Vautier 29, 1000 Brussels, Belgium
[8] Institute of Chemical Technology, Prague, Technická 5, CZ−16628, Prague 6, Czech Republic
[9] Institute of Rock Structures and Mechanics ASCR, v.v.i., V Holešovičkách 41, CZ−18209, Prague 8, Czech Republic

[*Received 18 February 2013; Accepted 25 March 2013; AE: S. Krivovichev*]

ABSTRACT

Leydetite, monoclinic $Fe(UO_2)(SO_4)_2(H_2O)_{11}$ (IMA 2012−065), is a new supergene uranyl sulfate from Mas d'Alary, Lodève, Hérault, France. It forms yellow to greenish, tabular, transparent to translucent crystals up to 2 mm in size. Crystals have a vitreous lustre. Leydetite has a perfect cleavage on (001). The streak is yellowish white. Mohs hardness is ~2. The mineral does not fluoresce under long- or short-wavelength UV radiation. Leydetite is colourless in transmitted light, non-pleochroic, biaxial, with α = 1.513(2), γ = 1.522(2) (further optical properties could not be measured). The measured chemical composition of leydetite, FeO 9.28, MgO 0.37, Al_2O_3 0.26, CuO 0.14, UO_3 40.19, SO_3 21.91, SiO_2 0.18, H_2O 27.67, total 100 wt.%, leads to the empirical formula (based on 21 O a.p.f.u.), $(Fe_{0.93}Mg_{0.07}Al_{0.04}Cu_{0.01})_{\Sigma 1.05}(U_{1.01}O_2)(S_{1.96}Si_{0.02})_{\Sigma 1.98}O_8(H_2O)_{11}$. Leydetite is monoclinic, space group $C2/c$, with a = 11.3203(3), b = 7.7293(2), c = 21.8145(8) Å, β = 102.402(3)°, V = 1864.18(10) Å^3, Z = 4, and D_{calc} = 2.55 g cm^{-3}. The six strongest reflections in the X-ray powder diffraction pattern are [d_{obs} in Å (I) (hkl)]: 10.625 (100) (002), 6.277 (1) ($\bar{1}$11), 5.321 (66) (004), 3.549 (5) (006), 2.663 (4) (008), 2.131 (2) (0 0 10). The crystal structure has been refined from single-crystal X-ray diffraction data to R_1 = 0.0224 for 5211 observed reflections with [$I > 3\sigma(I)$]. Leydetite possesses a sheet structure based upon the protasite anion topology. The sheet consists of UO_7 bipyramids, which share four of their equatorial vertices with SO_4 tetrahedra. Each SO_4 tetrahedron, in turn, shares two of its vertices with UO_7 bipyramids. The remaining unshared equatorial vertex of the bipyramid is occupied by H_2O, which extends hydrogen bonds within the sheet to one of a free vertex of the SO_4 tetrahedron. Sheets are stacked perpendicular to the c direction. In the interlayer, Fe^{2+} ions and H_2O groups link to the sheets on either side via a network of hydrogen bonds. Leydetite is isostructural with the synthetic compound $Mg(UO_2)(SO_4)_2(H_2O)_{11}$. The name of the new mineral honours Jean Claude Leydet (born 1961), an amateur mineralogist from Brest (France), who discovered the new mineral.

* E-mail: plasil@fzu.cz
DOI: 10.1180/minmag.2013.077.4.03

Keywords: leydetite, new mineral, uranyl sulfate, oxidation zone, crystal structure, Raman spectroscopy, infrared spectroscopy, Mas d′Alary, Lodève.

Introduction

Twenty uranyl sulfate minerals are currently known. They are rare, but relatively widespread, due to the common association of sulfide minerals, such as pyrite and chalcopyrite with uraninite. Among the uranyl sulfate minerals only one, deliensite (Vochten *et al.*, 1997; Plášil *et al.*, 2012*a*), contains Fe^{2+} as an essential constituent. Here, we present the description of the new mineral leydetite, a uranyl sulfate with medium sized cations (Strunz class 07.EB) and the second uranyl sulfate containing Fe^{2+} as an essential constituent. The new mineral and the name were approved by the Commission on New minerals, Nomenclature and Classification of the IMA (IMA2012−065). It is named in honour of Jean-Claude Leydet (born 1961), an amateur mineralogist and mineral collector from Brest, France. Jean-Claude Leydet is especially known for his studies of uranium-bearing minerals (Boisson and Leydet, 1998*a*,*b*; Leydet, 2006) and, in particular, those of the Mas d'Alary deposit (Henriot and Leydet, 1998). In 1994 he discovered the new mineral deliensite (Vochten *et al.*, 1997). In the same year he collected the new mineral described herein and named in his honour. The holotype specimen of leydetite is deposited in the collections of the Musée Cantonal de Géologie, Lausanne, Switzerland, registration number MGL 92661.

Occurrence

Leydetite was found at the Mas d'Alary uranium deposit, Lodève, Hérault, France (43º42′33″N; 03º20′12″E). The deposit was opened and exploited as an open pit from June 1984 to July 1992 (Bavoux and Guiollard, 1999). Uranium ore is found in grey Autunian sandstones, pelites and conglomerates. Local remobilization of U mineralization along fault zones is common in the deposit. Due to major tectonic events in the area, U-deposits in the Permian Lodève basin show a complex evolution with at least three U-mobilization stages, culminating with the recent alteration by oxygenated surface and subsurface waters, down to 30 m depth at Mas d'Alary (Deliens *et al.*, 1990; Lancelot *et al.*, 1995). Leydetite probably formed during this last stage. Associated minerals include abundant pyrite, less abundant uraninite (which however forms omnipresent inclusions in coal), calcite, quartz, unspecified clay minerals, gypsum and deliensite.

Physical and optical properties

Leydetite occurs as pale yellow to greenish, tabular, transparent to translucent crystals, up to 2 mm in size (Fig. 1). Crystals form multiple intergrowths. The Mohs hardness of leydetite is ~2. A density of 2.55 g cm^{-3} was calculated using the empirical formula. Leydetite floats in diodomethane with ρ = 3.32 g cm^{-3}. Leydetite is non-fluorescent under short- or long-wavelength UV radiation. The streak is yellowish white. Leydetite forms transparent to translucent crystals with a strong vitreous lustre. Leydetite is brittle and crystals exhibit excellent cleavage on (001). Intimate intergrowths of the crystals, polysynthetic twinning and a perfect cleavage did not allow feasible measurements of complete optical properties. Leydetite is colourless and biaxial; refractive indices were measured on fragments with a perfect cleavage on (001), α' = 1.513(2) and γ' = 1.522(2) (590 nm) with birefringence of 0.009. However, the absence of any crystal fragment with refractive indices n > 1.523 or n < 1.512 indicates that the measured refractive indices α' and γ' are close to α and γ.

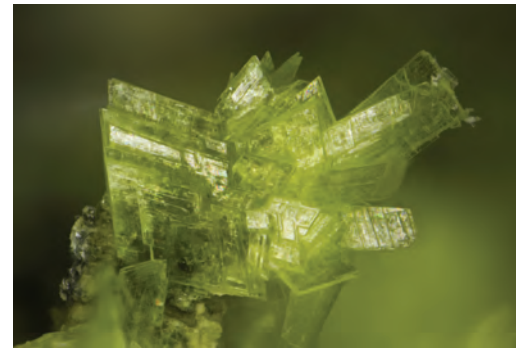

Fig. 1. Aggregate of leydetite crystals from Mas d'Alary, Lodève, France. The dominating faces are {001}, then {010} and {100}. Faces {101} and {011} occur also (and their symmetrically related equivalents). Field of view 2.5 mm. Photo by V. Bourgoin.

Hence, to calculate the Gladstone-Dale compatibility, at least as a best estimate, an average between α and γ refractive indices was taken as the β index, giving a calculated value of 1.518. The Gladstone-Dale compatibility index (Mandarino, 1981), calculated using the above-mentioned values and a density of 2.55 g cm^{-3}, is 0.016 (superior). The value of $2V_{calc}$ is then −83º (the mineral is probably biaxial positive). Leydetite dehydrates readily in dry air, becoming opaque and changing colour from yellow-green to orange-yellow.

Chemical composition

The chemical composition of leydetite was determined using a Cameca SX100 electron microprobe operating in the wavelength-dispersive mode with an acceleration voltage of 15 kV, beam current of 4 nA, and 15 μm beam diameter. The following X-ray lines and standards were selected to minimize line overlaps: Fe$K\alpha$ (hematite); Cu$L\alpha$ (lammerite); Mg$K\alpha$ (Mg_2SiO_4); Al, Si$K\alpha$ (sanidine); U$M\alpha$ (metallic U), S$K\alpha$ ($SrSO_4$). Peak counting times were 10−20 s and the counting time for background was 50% of the peak. The raw data were converted to element concentrations using the PAP routine (Pouchou and Pichoir, 1985).

Leydetite shows homogeneous chemical composition (Table 1) and its empirical formula (based on 21 O a.p.f.u.) is $(Fe_{0.93}Mg_{0.07}Al_{0.04}Cu_{0.01})_{\Sigma 1.05}(U_{1.01}O_2)(S_{1.96}Si_{0.02})_{\Sigma 1.98}O_8(H_2O)_{11}$. The simplified formula is $Fe(UO_2)(SO_4)_2(H_2O)_{11}$, which requires FeO 10.03, UO_3 39.98, SO_3 22.34, H_2O 27.65, total 100 wt.%. Leydetite is readily soluble in 10% HCl. On addition of KSCN, no colouration appeared, so it can be concluded the mineral does not contain any Fe^{3+}.

Infrared and Raman spectroscopy

The Raman spectrum (Fig. 2) of a leydetite crystal was collected using a DXR dispersive Raman spectrometer (ThermoElectron corp.) mounted on a confocal Olympus microscope (100 × objective) in the range 50−6400 cm^{-1} (with a resolution of 2 cm^{-1}). The Raman signal was excited by a 532 nm laser and detected by a CCD detector. Experimental parameters: exposure time, 10 s; number of exposures, 32; grating, 400 lines mm^{-1}; spectrograph aperture, 50 μm slit; laser power level: 2.5 mW. The infrared (IR) spectrum (Fig. 3) was collected using the ATR technique on a Nicolet 6700 FTIR spectrometer coupled to a Continuum microscope. The spectrum was collected from 4000−650 cm^{-1} with a resolution of 5 cm^{-1}. Spectra were processed (background correction, fitting) using the OMNIC Spectral tool software v.7.3 (ThermoElectron Corp.). We based our interpretations of both Raman and IR spectra on those presented by Čejka (1999, 2004, 2007), Volod'ko *et al.* (1965, 1981), Nakamoto (1986), Lane (2007) and Majzlan *et al.* (2011).

From a spectroscopic point of view, monoclinic leydetite contains in the primitive unit cell (Wigner-Seitz cell, or the first Brillouin zone) two

TABLE 1. Chemical composition (wt.%) of leydetite.

	Mean	Range	SD	Mean (normalized to 100 wt.%)		a.p.f.u.
FeO	10.88	10.65−11.10	0.20	9.28	Fe	0.93
CuO	0.16	0.00−0.31	0.13	0.14	Cu	0.01
MgO	0.43	0.25−0.55	0.11	0.36	Mg	0.07
Al_2O_3	0.31	0.11−0.46	0.12	0.26	Al	0.04
SiO_2	0.21	0.10−0.40	0.10	0.18	SiO_4	0.02
SO_3	25.68	24.07−26.88	1.02	21.91	SO_4	1.96
UO_3	47.10	46.01−47.89	0.65	40.19	UO_2^{2+}	1.01
H_2O*	32.65	31.90−33.64	0.62	27.67	H_2O	11.00
Total	117.40	114.63−120.68		100.00		

* H_2O in wt.% was calculated based on the content of 11 H_2O in the crystal structure of leydetite.

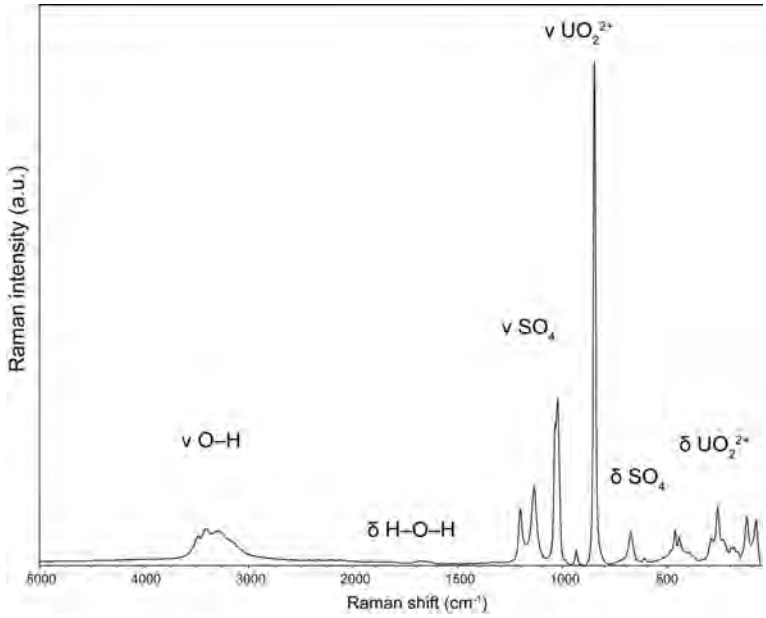

FIG. 2. Raman spectrum of leydetite.

Fe, two U and two S atoms. Lowering of symmetry of the tetrahedral SO_4 groups may lead to the activation of all modes in Raman and IR and also to the splitting of the degenerate ν_2 (δ), ν_3 and ν_4 (δ) vibrations. We observed an unusual splitting of Raman bands attributed to the ν_1 symmetric UO_2^{2+} stretching mode, which may be explained in the way reported by Volod'ko *et al.* (1965) for sodium uranyl acetate. Polarized Raman spectra and factor-group analysis would be required to understand more fully the cause of the splitting, but this is beyond the aim of the current paper.

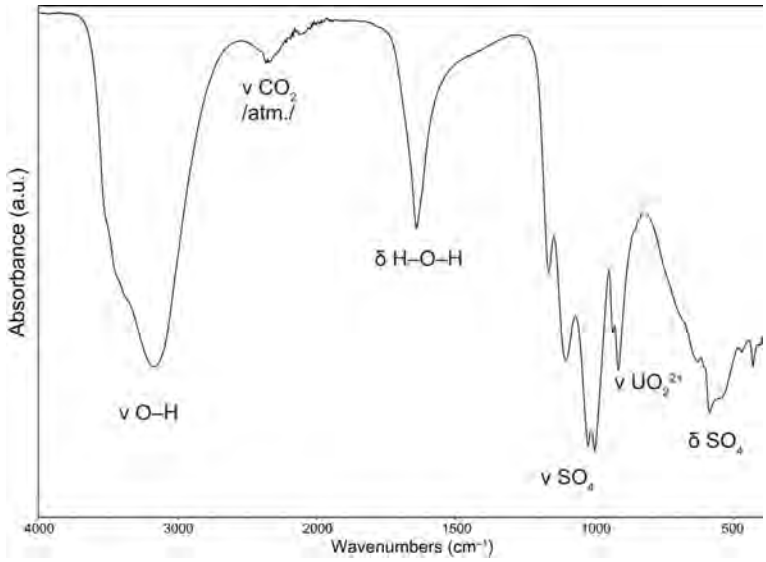

FIG. 3. IR spectrum of leydetite.

Raman bands at 3492, 3404, 3237 and 3130 cm^{-1} and IR bands at 3526, 3461, 33376 and 3169 cm^{-1} are assigned to ν(O−H) stretching vibrations of symmetrically non-equivalent H_2O molecules. According to Libowitzky's correlation (Libowitzky, 1999), O−H···O hydrogen-bond lengths, inferred from the frequencies of the observed vibrational bands, vary approximately in the range 2.82−2.69 Å. This range matches closely the values obtained from X-ray diffraction (~2.97−2.69 Å). The shoulder at 2927 cm^{-1} may be caused by organic impurities. Infrared bands at 2362 and 2345 cm^{-1} are artefacts due to atmospheric CO_2. Two Raman bands at 1679 and 1649 cm^{-1} and an IR band at 1641 cm^{-1} are related to the ν_2(H−O−H) bending vibrations of H_2O molecules.

Raman bands at 1203, 1180, 1150, 1139, 1135, 1113 and 1099 cm^{-1} (1166 and 1104 cm^{-1} in IR) are attributed to the split triply degenerate ν_3 antisymmetric stretching vibrations of SO_4. Bands at 1038, 1030, 1023 and 1015 cm^{-1} (1024 and 1001 cm^{-1} in IR) are attributable to the ν_1 symmetric stretching vibrations of SO_4 groups.

Raman bands at 937 and 930 cm^{-1} (in IR at 935 and 916 cm^{-1}) are assigned to the ν_3 antisymmetric stretching vibrations of UO_2^{2+} and those at 858, 851, 846, 843, 836 and 828 cm^{-1} to ν_1 symmetric stretching modes of UO_2^{2+}. In the IR spectrum no band that may be attributed to symmetric stretching of UO_2^{2+} was observed. According to Bartlett and Cooney (1989), U−O bond lengths, inferred from the frequencies of UO_2^{2+} stretching vibrations, vary in the range from 1.75 to 1.78 Å (for IR, 1.76 and 1.77 Å). This corresponds with those obtained from the present structure determination.

Raman bands at 686, 675, 666 and 608 cm^{-1} (IR at 630 and 588 cm^{-1}) are related to split triply degenerate ν_4 (δ) SO_4 bending vibrations, and those at 485, 464, 443 and 420 cm^{-1} (IR at 472 and 432 cm^{-1}) to split doubly degenerate ν_1 (δ) SO_4 bending vibrations. The reason for the increased number of observed Raman bands may

TABLE 2. Summary of data-collection conditions and refinement parameters for leydetite.

Ideal structural formula	$Fe[(UO_2)(SO_4)_2](H_2O)_{11}$
Unit-cell parameters (based on 6174 reflections)	
a, *b*, *c* (Å)	11.3203(3), 7.7293(2), 21.8145(8)
β (º)	102.402(3)
V (Å^3)	1864.18(10)
Z	4
Temperature (K)	293
Wavelength	Mo*K*α, 0.71073 Å
Crystal dimensions (mm)	0.45 × 0.22 × 0.05
Collection mode, frame width, count. time	ω scans, 1.0º, 7 s
Limiting θ angles (º)	3.21−29.38
Limiting Miller indices	$-15 \leqslant h \leqslant 15$, $-10 \leqslant k \leqslant 10$, $-27 \leqslant l \leqslant 28$
No. of reflections measured	10504
No. of unique reflections	8853
No. of observed reflections (criterion)	5211 [$I_{obs} > 3\sigma(I)$]
R_{int}	0.0403
Absorption correction (mm^{-1}), T_{min}/T_{max}	9.76, 0.206/0.646
F_{000}	1358
Refinement by *Jana2006* on F^2	
Space group	*C*2/*c*
Parameters refined, restraints, constraints	150, 10, 11
R_1, wR_2 (obs)	0.0224, 0.0238
R_1, wR_2 (all)	0.0274, 0.0251
GOF obs/all	1.19/1.20
$\Delta\rho_{min}$, $\Delta\rho_{max}$ (e Å^{-3})	−1.01, 1.51
Weighting scheme	$w = 1/(\sigma^2(F) + 0.0001F^2)$

TABLE 3. Atom positions and displacement parameters (U_{iso}/U_{eq}, in Å^2) for leydetite.

	x/*a*	*y*/*b*	*z*/*c*	U_{iso}/U_{eq}	U_{11}	U_{22}	U_{33}	U_{12}	U_{13}	U_{23}
U	0.5	0.20875(2)	0.25	0.01487(6)	0.01011(10)	0.01244(10)	0.02275(11)	0	0.00508(7)	0
Fe†	0	0	0	0.0274(3)	0.0332(5)	0.0233(5)	0.0259(5)	0.0022(4)	0.0069(4)	0.0004(3)
S	0.19154(8)	0.36898(11)	0.21074(4)	0.0191(3)	0.0162(4)	0.0150(4)	0.0280(5)	0.0018(4)	0.0092(4)	0.0019(4)
O1	-0.0777(3)	0.2296(4)	0.02715(17)	0.0416(12)	0.058(2)	0.0334(17)	0.038(2)	0.0166(16)	0.0211(17)	0.0041(15)
O2	0.4650(2)	0.2066(3)	0.16723(13)	0.0240(9)	0.0233(14)	0.0263(15)	0.0230(14)	0.0026(12)	0.0064(11)	0.0041(11)
O3	-0.1114(3)	–0.1552(5)	0.04473(16)	0.0404(12)	0.043(2)	0.0467(19)	0.0316(18)	0.0024(17)	0.0083(16)	0.0110(15)
O4	0.1222(3)	0.2179(4)	0.18393(15)	0.0339(11)	0.0395(18)	0.0283(16)	0.0358(17)	–0.0132(14)	0.0124(14)	–0.0086(13)
O5	0.6236(2)	–0.0398(3)	0.25242(13)	0.0238(9)	0.0171(13)	0.0222(14)	0.0346(15)	0.0059(11)	0.0116(11)	0.0018(11)
O6	0.1344(3)	0.0165(5)	0.08208(16)	0.0431(12)	0.046(2)	0.045(2)	0.0334(19)	0.0158(17)	–0.0020(16)	–0.0112(15)
O7	0.8178(3)	0.2807(4)	0.12750(15)	0.0352(11)	0.042(2)	0.0335(18)	0.0300(18)	–0.0072(15)	0.0086(15)	–0.0005(14)
O8	0.3064(2)	0.3136(3)	0.25264(14)	0.0273(9)	0.0156(14)	0.0271(15)	0.0414(17)	0.0067(11)	0.0113(12)	0.0054(12)
O9	0.1569(3)	0.4684(5)	0.03601(17)	0.0449(13)	0.054(2)	0.0353(19)	0.042(2)	–0.0119(16)	0.0032(18)	–0.0002(16)
O10	0.2146(3)	0.4834(4)	0.16201(14)	0.0332(10)	0.0401(18)	0.0270(15)	0.0362(17)	0.0003(13)	0.0164(13)	0.0097(13)
O11	0.5	0.5186(5)	0.25	0.0424(19)	0.038(3)	0.016(2)	0.085(4)	0	0.040(2)	0
H1	0.779(5)	0.211(6)	0.144(2)	0.0422*						
H2	0.460(5)	0.572(7)	0.266(2)	0.0509*						
H3	0.844(5)	0.344(6)	0.155(2)	0.0422*						
H4	–0.111(5)	0.317(6)	0.002(2)	0.05*						
H5	0.123(5)	0.077(7)	0.108(2)	0.0517*						
H6	0.160(5)	0.468(7)	0.073(2)	0.0539*						
H7	–0.091(5)	–0.185(6)	0.085(2)	0.0485*						
H8	–0.101(5)	0.239(7)	0.061(2)	0.05*						
H9	–0.185(4)	–0.122(7)	0.039(2)	0.0485*						
H10	0.124(5)	0.383(6)	0.021(2)	0.0539*						
H11	0.192(4)	–0.043(7)	0.091(2)	0.0517*						

† refined occupancy for the Fe atom is 0.981(4).
* refined with U_{iso} = 1.2; *U_{eq} of the parent O atom.

be the same as for the case of SO_4 stretching vibrations, but some of these bands may also be related to libration modes of H_2O molecules.

Raman bands at 538, 522 and 504 cm^{-1} are assigned to ν ($U-O_{ligand}$) stretching vibrations and librations of H_2O molecules. Raman bands at 394 and 373 cm^{-1} may be also attributed to the ν ($U-O_{ligand}$) stretching vibrations, and Raman bands at 290, 260, 236 and 223 cm^{-1} to split doubly degenerate ν_2 (δ) $(UO_2)^{2+}$ bending vibrations. Raman bands at 196, 182, 165, 138, 123, 116, 102, 89, 77 and 65 cm^{-1} are lattice modes.

Crystal structure of leydetite

Single-crystal X-ray diffraction

An untwinned fragment of leydetite, having dimensions of 0.16 mm × 0.06 mm × 0.02 mm was examined using an Oxford Diffraction Gemini single-crystal diffractometer with an Enhance-Mo collimator and Atlas CCD detector using monochromatized Mo*K*α radiation from a sealed X-ray tube. The unit cell was refined from 5177 reflections by the least-squares algorithm of the *CrysalisPro* package (Agilent Technologies, 2012) giving a monoclinic cell with a = 11.3203(3), b = 7.7293(2), c = 21.8145(8) Å, β = 102.402(3)º, V = 1864.18(10) $Å^3$, and Z = 4. Analysis of the diffraction frames after data collection revealed no additional diffraction peaks that might be present due to twinning. From 8914 measured reflections, 2345 were unique and 2159 were observed with the criterion [$I_{obs} > 3\sigma(I)$]. Data were corrected for Lorentz, polarization and background effects; a combined correction, multi-scan and analytical (Clark and Reid, 1997), for absorption effects was applied (*CrysAlis* RED, Agilent Technologies, 2012), leading to R_{int} = 0.0403. A summary of the data collection, crystallographic data and refinement is given in Table 2.

The crystal structure of leydetite (Table 3) was solved by the charge-flipping algorithm implemented in the *Superflip* program (Palatinus and Chapuis, 2007) and subsequently refined using the *Jana2006* software (Petříček *et al.*, 2006) with full-matrix least-squares refinement based on F^2. The reflection conditions and statistics clearly indicated the monoclinic space group *C*2/*c*. This space group was also suggested by the *Superflip* program, based on the symmetry operators deduced from the flipped electron density. All atom types except hydrogen atoms were refined anisotropically. Hydrogen atoms were treated using soft constraints on bond lengths, 0.90 Å with a constraint weight of (0.02), resulting in $D-H$ lengths from 0.76(6) to 0.90(5) Å (Table 4), and their isotropic displacement parameters were set to $1.2U_{eq}$ of the parent (donor) O atoms. The refinement converged with the final indices of agreement R_1 = 0.0224, wR_2 = 0.0238 for 2159 observed reflections with GOF = 1.19. On the basis of the refined interatomic distances (Table 5), the bond-valence analysis (Table 6) was performed following the procedure of Brown (1981, 2002).

TABLE 4. Hydrogen-bond geometry (Å, º) in the crystal structure of leydetite.

Bond	D−H	H···A	D···A	D−H···A angle
O7−H1···O10^{x}	0.82(5)	1.98(5)	2.755(5)	158(5)
O11−H2···O4^{xiii}	0.76(6)	1.93(6)	2.687(4)	172(5)
O7−H3···O5^{xiv}	0.79(5)	2.16(5)	2.912(4)	159(5)
O1−H4···O9^{vi}	0.90(5)	1.88(5)	2.760(5)	166(4)
O6−H5···O4	0.77(5)	1.98(5)	2.741(5)	169(5)
O9−H6···O10	0.80(4)	1.91(4)	2.688(5)	163(6)
O3−H7···O2^{viii}	0.88(4)	1.97(4)	2.835(4)	169(5)
O1−H8···O7^{v}	0.85(5)	1.90(6)	2.732(6)	168(5)
O3−H9···O9^{viii}	0.85(4)	1.91(5)	2.759(5)	173(5)
O9−H10···O3^{ii}	0.79(5)	2.25(5)	2.973(5)	151(6)
O6−H11···O7^{viii}	0.79(5)	2.01(5)	2.780(5)	166(5)

Symmetry codes: (ii) $-x$, $-y$, $-z$; (v) $x-1$, y, z; (vi) −x, $-y+1$, $-z$; (viii) $x-1/2$, $y-1/2$, z; (x) $x+1/2$, $y-1/2$, z; (xiii) $-x+1/2$, $y+1/2$, $-z+1/2$; (xiv) $-x+3/2$, $y+1/2$, $-z+1/2$.

TABLE 5. Selected interatomic distances (in Å) for leydetite.

U−O2	1.763(3)	Fe−O1	2.121(4)
U−O2^{i}	1.763(3)	Fe−O1^{ii}	2.121(4)
U−O5	2.371(3)	Fe−O3	2.124(4)
U−O5^{i}	2.371(3)	Fe−O3^{ii}	2.124(4)
U−O8	2.349(3)	Fe−O6	2.089(3)
U−O8^{i}	2.349(3)	Fe−O6^{ii}	2.089(3)
U−O11	2.395(4)	<Fe−O>	2.11
<U−O_{eq}>	2.37		

S−O4	1.458(3)
S−O5^{iii}	1.488(3)
S−O8	1.482(3)
S−O10	1.449(3)
<S−O>	1.47

Symmetry codes: (i) $-x+1$, y, $-z+1/2$; (ii) $-x$, $-y$, $-z$; (iii) $x-1/2$, $y+1/2$, z.

Description of the crystal structure

Structure solution and subsequent refinement proved that leydetite is isostructural with the synthetic compound $Mg(UO_2)(SO_4)_2(H_2O)_{11}$ reported by Serezhkin *et al.* (1981). The current structure model for leydetite contains refined positions of hydrogen atoms, which were not determined in the earlier structure determination for the synthetic compound. The crystal structure of leydetite contains symmetrically unique U, Fe and S atoms, eleven distinct O atoms and eleven distinct H atoms in the asymmetric unit. The crystal structure is based upon protasite anion topology, with sheets of polyhedra containing triangles and pentagons (Burns 2005). These sheets arise from the linkage of uranyl pentagonal bipyramids with sulfate tetrahedra *via* shared vertices. Each pentagonal bipyramid is four-connected within the sheet. At the free vertex of the bipyramid, the H_2O group extends hydrogen bonds (O11−H2···O4) towards one of the free vertices of the sulfate tetrahedron (Figs 4 and 5). Sheets are parallel to {001}. In the interlayer, $Fe^{2+}(H_2O)_6$ octahedra and isolated H_2O groups are located. These link to one another and to the sheets on either side via a network of hydrogen bonds (Fig. 5).

Powder X-ray diffraction

Powder X-ray diffraction data for leydetite were obtained using a Bruker D8 Discover powder diffractometer equipped with a LynxEye detector and a primary double-crystal Si monochromator providing Cu$K\alpha_1$ radiation. X-ray powder diffraction data are listed in Table 7. Positions of diffraction maxima were obtained by profile fitting performed with *Xfit* software (Cheary and Coelho, 1997). The unit cell was refined with *Celref* software (Laugier and Bochu, 2003). The powder pattern of leydetite is strongly influenced by the preferred orientation of the type (00*l*), which

TABLE 6. Bond-valence analysis for leydetite.

	U	S	Fe	H1	H2	H3	H4	H5	H6	H7	H8	H9	H10	H11	ΣBV	
O1			0.35 × 2↓				0.70				0.74				1.79	O
O2	1.74 × 2↓									0.23					1.97	O
O3			0.35 × 2↓							0.72		0.74	0.17		1.98	O
O4		1.57			0.24			0.22							2.03	O
O5	0.54 × 2↓	1.44				0.18									2.16	O
O6			0.38 × 2↓					0.81						0.79	1.98	O
O7				0.78		0.79					0.24			0.22	2.07	O
O8	0.56 × 2↓	1.47													2.03	O
O9							0.25		0.78			0.24	0.79		2.04	O
O10		1.60		0.22					0.24						2.06	O
O11	0.52				0.82										2.14	O
	6.21	6.08	2.16	1.00	1.06	0.97	0.95	1.03	1.02	0.95	0.98	0.98	0.96	1.01		

Values are expressed in valence units (v.u.). Multiplicity indicated by × 2↓. U^{6+}−O bond strengths ($r_0 = 2.045$, $b = 0.51$) from Burns *et al.* (1997); S^{6+}−O and Fe^{2+}−O bond strengths from Brown and Altermatt (1985); H^{+}−O bond strengths after Brown (2002).

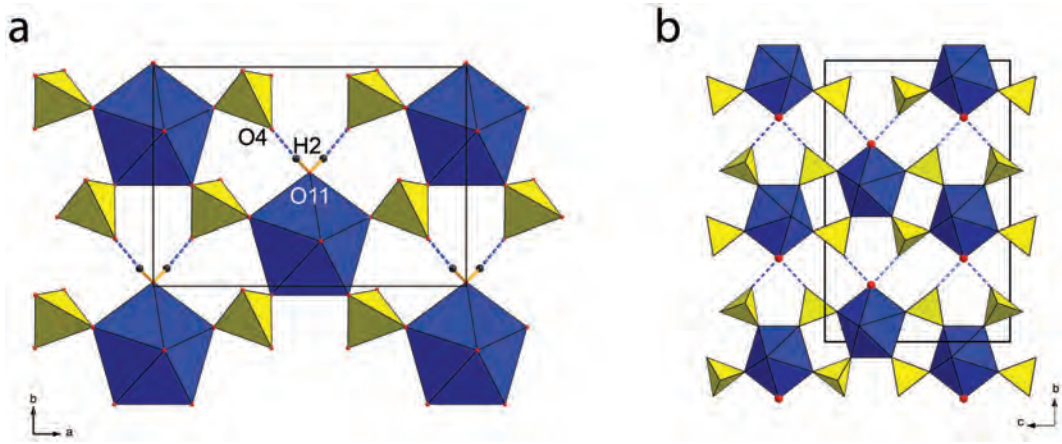

FIG. 4. (*a*) The sheet and hydrogen bonding in the structure of leydetite. (*b*) Infinite chains of polyhedra in the structure of $K_2[(UO_2)(SO_4)_2(H_2O)](H_2O)$ (Ling *et al.*, 2010). The H bonds (in the case of the compound proposed by Ling *et al*. (2010) only) are represented by dashed lines. The unit-cell edges are outlined.

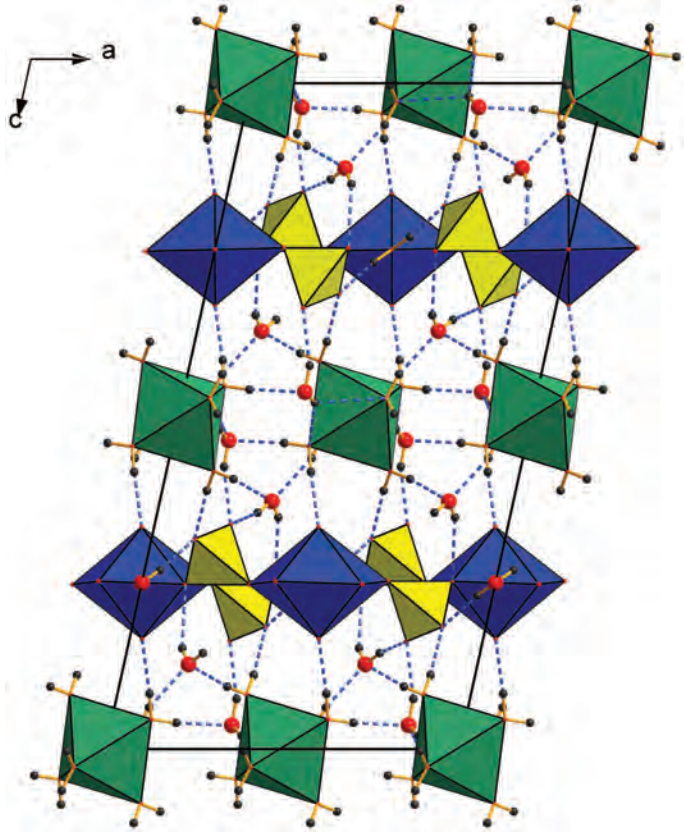

FIG. 5. The structure of leydetite possessing sheets of uranyl pentagonal bipyramids (blue) and sulfate tetrahedra (yellow), stacked along {001}. Octahedra of composition $Fe^{2+}(H_2O)_6$ (green) and an additional four H_2O groups are located in the interlayer. Hydrogen bonds are displayed as dashed blue lines, hydrogen atoms as black circles.

TABLE 7. Powder X-ray diffraction data (d_{hkl} in Å) for leydetite.

I_{obs}	I_{calc}	d_{obs}	d_{calc}	h	k	l	I_{obs}	I_{calc}	d_{obs}	d_{calc}	h	k	l
100.00	100	10.625	10.657	0	0	2	0.02	3	2.3305	2.3304	1	3	3
1.34	42	6.277	6.287	$\bar{1}$	1	1	0.10	3	2.3123	2.3138	$\bar{1}$	1	9
0.48	27	5.873	5.877	1	1	1	0.06	2	2.2289	2.2314	2	2	6
0.24	10	5.759	5.766	$\bar{1}$	1	2	0.08	1	2.2217	2.2223	3	1	6
0.16	15	5.524	5.527	2	0	0	0.15	4	2.2201	2.2206	2	0	8
66.05	52	5.321	5.329	0	0	4	0.05	5	2.1630	2.1627	$\bar{5}$	1	3
0.78	23	5.167	5.172	1	1	2	0.04	1	2.1494	2.1494	$\bar{4}$	2	5
0.64	37	5.042	5.047	$\bar{1}$	1	3	0.18	4	2.1335	2.1338	1	1	9
0.31	15	4.457	4.463	1	1	3	1.78	2	2.1309	2.1315	0	0	10
0.09	11	4.325	4.329	$\bar{2}$	0	4	0.19	5	2.1264	2.1257	4	2	2
0.30	24	3.755	3.757	$\bar{1}$	1	5	0.09	2	2.1208	2.1176	1	3	5
0.12	18	3.630	3.633	0	2	2	0.29	4	2.1110	2.1113	3	3	0
5.00	4	3.549	3.552	0	0	6	0.18	1	2.0767	2.0761	3	3	1
0.26	16	3.481	3.480	2	0	4	0.18	6	2.0513	2.0513	$\bar{3}$	3	4
0.05	1	3.392	3.395	0	2	3	0.09	1	1.9493	1.9489	1	1	10
0.72	24	3.387	3.388	$\bar{3}$	1	1	0.16	3	1.9197	1.9203	$\bar{1}$	1	11
0.20	4	3.348	3.351	1	1	5	0.15	2	1.8852	1.8850	3	3	4
0.02	1	3.337	3.332	$\bar{2}$	0	6	0.04	3	1.8782	1.8787	$\bar{2}$	2	10
0.18	15	3.264	3.265	$\bar{3}$	1	3	0.04	1	1.8705	1.8697	$\bar{6}$	0	4
0.26	8	3.189	3.190	$\bar{2}$	2	1	0.05	2	1.8679	1.8664	0	2	10
0.38	16	3.143	3.143	$\bar{2}$	2	2	0.09	2	1.8649	1.8644	0	4	3
0.15	9	3.078	3.078	2	2	1	0.07	3	1.7923	1.7922	1	1	11
0.22	6	3.034	3.035	$\bar{2}$	2	3	0.07	3	1.7839	1.7837	1	3	8
0.45	4	2.9456	2.9474	1	1	6	0.94	1	1.7761	1.7762	0	0	12
0.05	2	2.9118	2.9104	$\bar{3}$	1	5	0.04	2	1.7656	1.7652	4	2	6
0.30	14	2.8846	2.8867	$\bar{1}$	1	7	0.04	2	1.7639	1.7639	$\bar{3}$	3	8
0.05	7	2.8256	2.8267	$\bar{4}$	0	2	0.08	1	1.7366	1.7372	2	4	3
0.05	4	2.8084	2.8102	3	1	3	0.04	1	1.6895	1.6893	2	4	4
0.08	3	2.7673	2.7686	2	2	3	0.04	1	1.6373	1.6377	$\bar{2}$	2	12
0.08	4	2.7064	2.7068	$\bar{2}$	2	5	0.04	<1	1.6178	1.6173	5	3	2
0.10	2	2.7030	2.7037	$\bar{3}$	1	6	0.05	1	1.5942	1.5942	2	0	12
4.26	5	2.6631	2.6644	0	0	8	0.37	1	1.5225	1.5225	0	0	14
0.07	2	2.6209	2.6212	1	1	7	0.04	1	1.5042	1.5043	4	2	9
0.06	5	2.5858	2.5862	2	2	4	0.05	1	1.4498	1.4500	$\bar{3}$	3	12
0.08	2	2.5458	2.5454	4	0	2	0.17	<1	1.3324	1.3322	0	0	16
0.06	4	2.5081	2.5090	1	3	0	0.08	<1	1.1843	1.1842	0	0	18
0.01	4	2.4049	2.4029	$\bar{1}$	3	3	0.06	<1	1.0660	1.0657	0	0	20

5–100º2θ Cu$K\alpha$, step size 0.01º, counting time 4 s step^{-1}, sample was rotated (frequency 0.5 s^{-1}).

is caused by the excellent cleavage of the crystals. Diffraction maxima were indexed in accordance with the calculated values of intensities obtained from the structure model and calculated by the PowderCell program (Kraus and Nolze, 1996). Refined unit-cell parameters from the powder data are given in Table 8.

Discussion

The structures of two synthetic uranyl sulfates are based upon the same sheet topology as leydetite. These are $[(UO_2)(SO_4)_2]H_2(H_2O)_5$ (Alcock *et al.*, 1982) and $K_2[(UO_2)(SO_4)_2](H_2O)_2$ (Niinistö *et al.*, 1979). The latter is particularly interesting in that its possible occurrence in nature cannot be excluded. We speculate that it may occur in acid environments with a high activity of K^+, as does adolfpateraite, $K[(UO_2)(SO_4)(OH)(H_2O)]$ (Plášil *et al.*, 2012*b*), particulary considering the similar value of the charge deficiency per anion (Schindler and Hawthorne, 2008) of the structural units of these two compounds. Interestingly, the basic sheet motif in leydetite,

TABLE 8. Refined unit-cell parameters for leydetite and for synthetic $Mg(UO_2)(SO_4)_2(H_2O)_{11}$.

	Leydetite, Mas d'Alary Single-crystal; this study	Leydetite, Mas d'Alary Powder; this study	$Mg(UO_2)(SO_4)_2(H_2O)_{11}$ Single-crystal; Serezhkin *et al.* (1981)
a	11.3203(3)	11.319(3)	11.334(6)
b	7.7293(2)	7.723(1)	7.715(3)
c	21.8145(8)	21.826(3)	21.709(9)
β	102.402(3)	102.41(2)	102.22(6)
V	1864.18(10)	1864.7(6)	1855.3

$[(UO_2)(SO_4)_2(H_2O)]^{2-}$, is similar to that of another synthetic compound, $K_2[(UO_2)(SO_4)_2(H_2O)](H_2O)$, prepared by Ling *et al.* (2010). Sheet linkages are compared in Figs 4*a* and *b*. The sheets are topological isomers of the sheet in leydetite (Fig. 4*a*) which is more highly polymerized than that in $K_2[(UO_2)(SO_4)_2(H_2O)](H_2O)$, where the alternating up-down orientation of pentagonal bipyramids (Fig. 4*b*) prevents the chains from polymerizing further to form sheets.The orientation of the tetrahedral elements in the chain structure of $K_2[(UO_2)(SO_4)_2(H_2O)](H_2O)$ also offers the possibility of geometrical isomerism.

Leydetite is known only from the type locality. However, Plášil *et al.* (2012*a*) described an unnamed mineral having a very similar chemical composition from the L'Ecarpière mine, Gétigné, Loire Atlantique, France. The unnamed phase was found to be the part of a deliensite sample, forming crusts overgrown by deliensite. The unnamed phase has the empirical formula: $(Fe_{0.71}Mg_{0.20}Zn_{0.08}Mn_{0.02})_{\Sigma 1.01}(UO_2)_{1.01}[(SO_4)_{1.98}(SiO_4)_{0.02}]_{\Sigma 2.00}(H_2O)_n$ (calculated as the mean of 5 point analysis on the basis of 2 S + Si a.p.f.u.). Based on this result we conclude that this phase is equivalent to leydetite.

Acknowledgements

The authors thank Jean-Claude Leydet (Brest) for providing us with the material for study. We also thank Vincent Bourgoin for providing photomicrographs of leydetite samples. Referees Tony Kampf and Igor Pekov are thanked for thorough reviews that helped improve the manuscript. This work was supported by the Premium Academiae and a grant of the Czech Science Foundation (P204/11/0809) to MD, KF and JP. Further support was provided by EU-project "Research group for radioactive waste repository and nuclear safety" (CZ.1.07/2.3.00/20.0052) to RŠ and MN, as well as a long-term project of the Ministry of Culture of the Czech Republic (MK00002327201) to JČ.

References

Agilent Technologies (2012) CrysAlis *CCD* and CrysAlis *RED*. Oxford Diffraction Ltd, Yarnton, Oxfordshire, UK.

Alcock, N.W., Roberts, M.M. and Brown, D. (1982) Actinide structural studies. Part 3. The crystal and molecular structures of $UO_2SO_4{\cdot}H_2SO_4{\cdot}5H_2O$ and $2NpO_2SO_4{\cdot}H_2SO_4{\cdot}4H_2O$. *Journal of the Chemical Society, Dalton Transactions*, 869–873.

Bartlett, J.R. and Cooney, R.P. (1989) On the determination of uranium-oxygen bond lengths in dioxouranium(VI) compounds by Raman spectroscopy. *Journal of Molecular Structure*, **193**, 295–300.

Bavoux, B. and Guiollard, P.-C. (1999) *L'uranium du Lodévois (Hérault)*. Saint-Pourcain, Sioule.

Boisson, J.-M. and Leydet, J.-C. (1998*a*) L'uranium et ses descendants. La Radioactivité. *Le Régne Minéral*, hors série **IV**, 13–36.

Boisson, J.-M. and Leydet, J.-C. (1998*b*) Les minéraux uranifères français. La Radioactivité. *Le Régne Minéral*, hors série **IV**, 37–60.

Brown, I.D. (1981) The bond-valence method: an empirical approach to chemical structure and bonding. Pp. 1–30 in: *Structure and Bonding in Crystals II* (M. O'Keeffe and A. Navrotsky, editors). Academic Press, New York, USA.

Brown, I.D. (2002) *The Chemical Bond in Inorganic Chemistry: The Bond Valence Model*. Oxford University Press, UK.

Brown, I.D. and Altermatt, D. (1985) Bond-valence parameters obtained from a systematic analysis of the inorganic crystal structure database. *Acta Crystallographica*, **B41**, 244–247, with updated parameters from http://www.ccp14.ac.uk/ccp/web-mirrors/i_d_brown/.

Burns, P.C. (2005) U^{6+} minerals and inorganic

compounds: insights into an expanded structural hierarchy of crystal structures. *The Canadian Mineralogist*, **43**, 1839–1894.

Burns, P.C., Ewing, R.C. and Hawthorne, F.C. (1997) The crystal chemistry of hexavalent uranium: polyhedron geometries, bond-valence parameters, and polymerization of polyhedra. *The Canadian Mineralogist*, **35**, 1551–1570.

Čejka, J. (1999) Infrared spectroscopy and thermal analysis of the uranyl minerals. Pp. 521–622 in: *Uranium: Mineralogy, Geochemistry and the Environment* (P.C. Burns and R. Finch, editors). Reviews in Mineralogy, **38**, Mineralogical Society of America, Washington DC.

Čejka, J. (2004) Vibrational spectroscopy of uranyl minerals – infrared and Raman spectra of uranyl minerals. I. Uranyl, UO_2^{2+}. *Bulletin mineralogicko-petrologického Oddělení Národního Muzea (Praha)*, **12**, 44–51 (in Czech).

Čejka, J. (2007) Vibrational spectra of uranyl minerals – infrared and Raman spectra of uranyl minerals. III. Uranyl sulphates. *Bulletin mineralogicko-petrologického Oddělení Národního Muzea (Praha)*, **14–15**, 40–46 (in Czech).

Cheary, R.W. and Coelho, A.A. (1997) XFIT and FOURYA. CCP14 Powder Diffraction Library, Engineering and Physical Sciences Research Council, Daresbury Laboratory, Warrington, UK (http://www.ccp14.ac.uk/tutorial/xfit-95/xfit.htm).

Clark, R.C. and Reid, J.S. (1995) The analytical calculation of absorption in multifaceted crystals. *Acta Crystallographica*, **A51**, 887–897.

Deliens, M., Henriot, O., Mathis, V. and Caubel, A. (1990) *Minéraux des gisements d'uranium du Lodévois*. Association française de Microminéralogie, Paris.

Henriot, O. and Leydet, J.-C. (1998) Le gisement de Mas d'Alary Village, Hérault, France. *Le cahier des Micromonteurs*, **2**, 13–26.

Kraus, W. and Nolze, G. (1996) POWDER CELL – a program for the representation and manipulation of crystal structures and calculation of the resulting X-ray powder patterns. *Journal of Applied Crystallography*, **29**, 301–303.

Lancelot, J., Briqueu, L., Respaut, J.-P. and Clauer, N. (1995) Géochimie isotopique des systèmes U-Pb/Pb-Pb et évolution polyphasée des gîtes d'uranium du Lodévois et du sud du Massif central. *Chronique de la Recherche Minière*, **521**, 3–18.

Lane, M.D. (2007) Mid-infrared emission spectroscopy of sulphate and sulphate-bearing minerals. *American Mineralogist*, **92**, 1–18.

Laugier, J. and Bochu, B. (2003) *CELREF: Unit Cell Refinement Program from Powder Diffraction Diagram*. Laboratoires des Matériaux et du Génie Physique, Ecole Nationale Supérieure de Physique de Grenoble (INPG), Grenoble, France.

Leydet, J.-C. (2006) Shinkolobwe, République Démocratique du Congo-cahier spécial: minéraux dédiés à des minéralogistes français ou à des localités françaises. *Le cahier des Micromonteurs*, **10**, 86–88.

Libowitzky, E. (1999) Correlation of O-H stretching frequencies and O–H···O hydrogen bond lengths in minerals. *Monatshefte für Chemie*, **130**, 1047–1059.

Ling, J., Sigmon, G.E., Ward, M., Roback, N. and Burns, P.C. (2010) Syntheses, structures, and IR spectroscopic characterization of new uranyl sulphate/selenate 1D-chain, 2D-sheet and 3D-framework. *Zeitschrift für Kristallographie*, **225**, 230–239.

Majzlan, J., Alpers, C.N., Koch, C.B., McCleskey, R.B., Myneni, S.C.B. and Neil, J.M. (2011) Vibrational, X-ray absorption, and Mössbauer spectra of sulfate minerals from the weathered massive sulfide deposit at Iron Mountain, California. *Chemical Geology*, **284**, 296–305.

Mandarino, J.A. (1981) The Gladstone-Dale relationship. IV. The compatibility concept and its application. *The Canadian Mineralogist*, **19**, 441–450.

Nakamoto, K. (1986) *Infrared and Raman Spectra of Inorganic and Coordination Compounds*. J. Wiley and Sons, New York.

Niinistö, L., Toivonen J. and Valkonen, J. (1979) Uranyl (VI) compounds. II. The crystal structure of potassium uranyl sulphate dihydrate $K_2UO_2(SO_4)_2{\cdot}2H_2O$. *Acta Chemica Scandinavica*, **A33**, 621–624.

Palatinus, L. and Chapuis, G. (2007) Superflip – a computer program for the solution of crystal structures by charge flipping in arbitrary dimensions. *Journal of Applied Crystallography*, **40**, 451–456.

Petříček, V., Dušek, M. and Palatinus, L. (2006) *Jana2006. The crystallographic computing system*. Institute of Physics, Prague, Czech Republic.

Plášil, J., Hauser, J., Petříček, V., Meisser, N., Mills, S.J., Škoda, R., Fejfarová, K., Čejka, J., Sejkora, J., Hloušek, J., Johannet, J.-M., Machovič, V. and Lapčák. L. (2012*a*) Crystal structure and formula revision of deliensite, $Fe[(UO_2)_2(SO_4)_2(OH)_2](H_2O)_7$. *Mineralogical Magazine*, **76**, 2837–2860.

Plášil, J., Hloušek, J., Veselovský, F., Fejfarová, K., Dušek, M., Škoda, R., Novák, M., Čejka, J., Sejkora, J. and Ondruš, P. (2012*b*) Adolfpateraite, $K(UO_2)(SO_4)(OH)(H_2O)$, a new uranyl sulphate mineral from Jáchymov, Czech Republic. *American Mineralogist*, **97**, 447–454.

Pouchou, J.L. and Pichoir, F. (1985) "PAP" (φ ρZ) procedure for improved quantitative microanalysis. Pp. 104–106 in: *Microbeam Analysis* (J.T.

Armstrong, editor). San Francisco Press, San Francisco, California, USA.

Schindler, M. and Hawthorne, F.C. (2008) The stereochemistry and chemical composition of interstitial complexes in uranyl-oxysalt minerals. *The Canadian Mineralogist*, **46**, 467–501.

Serezhkin, V.N., Soldatkina, M.A. and Efremov, V.A. (1981) Crystal structure of $Mg(UO_2)(SO_4)_2{\cdot}11H_2O$. *Journal of Structural Chemistry*, **22**, 454–457.

Vochten, R., Blaton, N. and Peeters, O. (1997) Deliensite, $Fe(UO_2)_2(SO_4)_2(OH)_2{\cdot}3H_2O$, a new ferrous uranyl sulphate hydroxy hydrate from Mas d'Alary, Lodève, Hérault, France. *The Canadian Mineralogist*, **35**, 1021–1025.

Volod'ko, L.V., Komyak, A.I. and Sleptsov, L.I. (1965) Infrared absorption spectrum of the sodium uranyl acetate single crystal. *Zhurnal Prikladnoi Spektroskopii*, **3**, 65–71.

Volod'ko, L.V., Komyak, A.I. and Umreyko, D.S. (1981) *Uranyl Compounds, Spectra and Structure*, vol. 1. Izdatelsvo BGU Minsk (in Russian).